Lidar systems testing considerations for field use

Helena Picmausová
Fraunhofer Institute of Optronics, System Technologies and Image Exploitation IOSB
Ettlingen, Germany;
University of Defence
Brno, Czech Republic
https://orcid.org/0000-0003-3683-7243

Jan Farlík
University of Defence
Brno, Czech Republic
https://orcid.org/0000-0001-7254-2405

Marc Eichhorn
Fraunhofer Institute of Optronics, System Technologies and Image Exploitation IOSB
Ettlingen, Germany;
Karlsruhe Institute of Technology
Karlsruhe, Germany
marc.eichhorn@iosb.fraunhofer.de

Christelle Kieleck
Fraunhofer Institute of Optronics, System Technologies and Image Exploitation IOSB
Ettlingen, Germany
christelle.kieleck@iosb.fraunhofer.de

***Abstract*— The aim of this paper is to offer a perspective on testing a commercially available lidar system in order to determine its suitability for various practical tasks including mapping, object recognition, and the potential in its coupling with another sensor, in this case a camera. Several mapping missions were carried out over the course of the experiment, with both the lidar and the camera mounted on an Unmanned Aircraft System. Aside from mapping ordinary objects like trees, vehicles, people, and ground elevation, a standardized test target was designed for the purposes of the experiment, and placed in detection area. Influence of external factors on system performance was evaluated, e.g. atmospheric conditions and material properties of scanned surfaces, especially their reflectivity. Post processing of obtained data was carried out, demonstrating the potential of overlaying multiple sensor data for easier object recognition, and an optimal use case for the system is suggested.**

Keywords*— *Sensors, lidar, Unmanned Aircraft Systems, 3D mapping, camera imaging, object detection

I. Introduction

In recent years, Lidar (light detection and ranging) has been an object of extensive research and development, with ever increasing prominence among active electro-optic sensors. With fields of application spanning from meteorology and geoscience to object identification, autonomous navigation, to aerospace and defence, the technology has also become increasingly accessible, affordable, and compact [1]-[4]. With the variety of solutions available on the market, it is important to choose an appropriate system for a given application, and keep limitations of technology in mind.

II. Lidar systems considerations

Several parameters need to be accurately calculated and tested to determine effective range and operational limitations of a lidar system. Usually, the main performance factors are the laser source – its output power, pulse length, and wavelength, update frequency of the positioning system and atmospheric conditions. One of the advantages of lidar is that unlike many passive sensors, it can function in low light conditions, and given an equivalent-sized optical aperture, higher resolution can be achieved thanks to a lower diffraction limit at shorter wavelengths [1], [11].

For lidar applications, among the most popular laser sources are diode pumped solid-state lasers, which allow for nanosecond-class pulse generation using Q switching, [7]. Thanks to their widespread availability and maturity, Nd3+:YAG doped lasers emitting at 1064 nm can be therefore encountered in lidar solutions, despite their relatively lower quantum efficiency [1], [10].

Another increasingly popular option is a diode-pumped fiber laser solution, which generally offers exceptional beam quality and resilience to mechanical shock due to the absence of free-space optics. Furthermore, lasers operating above 1550 nm wavelength are deemed ‚eye-safer‘, and also offer easy availability of components owing to telecommunication applications [5], [7].

Diode lasers operating around the 905 nm range are also often used in lidars, especially in the automotive industry, due to their compact size, low cost and good efficiency, and naturally, resolution is better with shorter wavelengths; but as they cannot store energy, their low pulse energies result in considerably shorter detection ranges [8], [9], [11].

Atmospheric conditions should also be taken into account when evaluating lidar performance results. Unlike atmospheric scattering, atmospheric absorption is wavelength specific for each air component, so a careful choice of wavelength can impact beam power decay on the two-way path to the target and back. Neither the 905 nm, 1064 nm, nor the 1550 nm range offer zero absorption. Atmospheric humidity is therefore a key factor when attempting any lidar measurement [10].

Illuminance is another key factor for lidar detection range, which is significantly reduced with higher ambient illuminance. Performance testing on a sunlit day (approx. 100 klx) reportedly results in a reduction of detection range to around 70% of values obtained during clear night conditions (0 klx), [12], [13].

III. Experiment

The experiment consisted of testing capabilities of a commercially available automotive-grade lidar system coupled with an RGB mapping camera, both coupled with an Inertial Measurement Unit (IMU) and mounted on a UAS (Unmanned Aircraft System), make DJI Matrice 300 RTK. A test area has been set up allowing for multiple mapping flights at various altitudes, and containing various sized targets and landscape elements such as ground elevation, tents, buildings, vehicles and trees.

The goals of the experiment included verification of the accuracy stated in the lidar datasheet, the influence of flight altitude, detection capabilities of both sensors (the lidar and the camera) of objects with various reflectance and their mutual data agreement.

Given the airborne mapping approach, an accurate positioning solution is crucial in this experiment, and although UAS navigation benefits from the advancement of global positioning system (GPS), the inertial navigation system (INS) measurements are key, making the IMU update frequency an important factor, as well as yaw, pitch, and angle/roll accuracy.

A. *Test target*

Aside from the above-mentioned terrain elements, test targets were designed, providing a measurement standard for the lidar resolution capability, as accuracy can be greatly improved by pre-acquired metric data, as reported in [6].

The experimental targets were a new original design created for the purpose of this experiment. They were 3D printed from materials with various reflectivity to determine the influence of colour and material as well as dimensions.

Figure 1 and Figure 2 show the two versions of the test target, each consisting of multiple cubes with side lengths of 1, 2, 4, and 8 cm, allowing for resolution testing of horizontal, vertical and depth/distance accuracy.

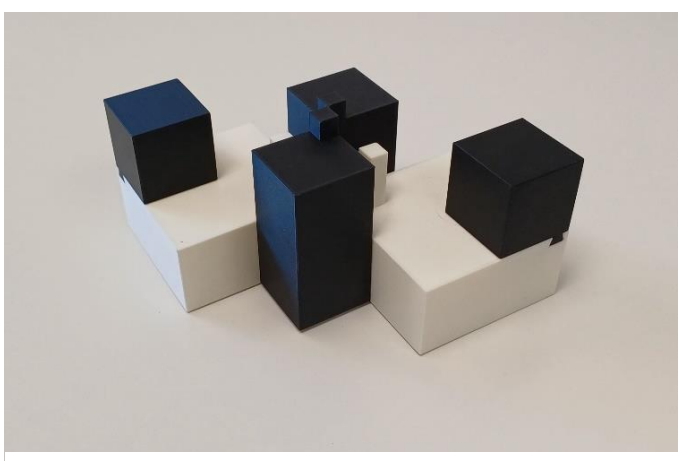

Fig. 1. Test target no. 1, consisting of low reflectivity black cubes and high reflectivity white cubes, providing high contrast.

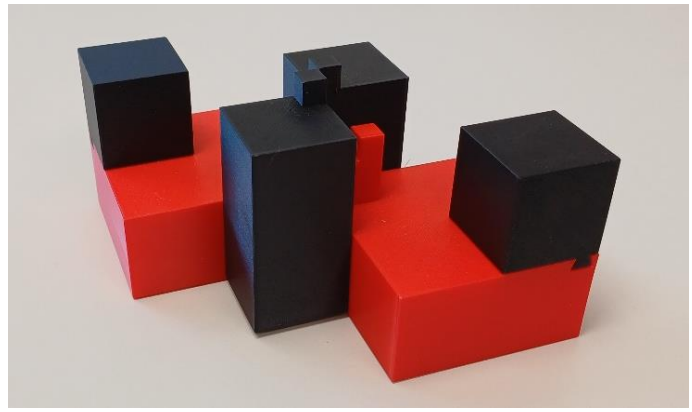

Fig. 2. Test target no. 2, combining low reflectivity black cubes and medium reflectivity red cubes, providing lower contrast.

B. *Lidar system specifications*

The manufacturer-declared specifications include the lidar ranging accuracy of 2-3 cm at a 100 m distance, 905 nm wavelength, 30 W system power, IMU update frequency of 200 Hz and a point return rate over 240,000 pts/s, with a detection range reaching over 400 m at 80% reflectivity, and the operating temperature range from -20° to 50° C. The software used offers flight route planning with flight track overlap and angle options, time-of-flight estimation, and postprocessing tools including an overlay of the acquired lidar data point cloud and photogrammetry images from the 20 MP, 1" CMOS camera.

C. *Flight conditions*

The test area was scanned during multiple mapping flights at 50 and 100 m altitude. The scanning area overlap was set to 20%

Fig. 3. A photo taken by the RGB camera from flight altitude of 50 m, with a clearly visible white tent, a few people standing on the walkway and a very small but visible target – circled in yellow and red, respectively.

for the 50 m, and at 50% for the 100 m flight. The experiment was carried out during clear weather conditions, calm wind, temperature of 18° C, humidity levels under 30%, in full daylight. A reference photo of target area is shown in Figure 3.

IV. Results

The results using both the lidar point cloud, and an overlay from photogrammetry can be seen below in Figure 4. It is worth noting that the side of the white tent hasn't been detected at all, likely due to the scanning incidence angle, a similar issue to one previously reported in [6], that can be sometimes ameliorated by energy balance normalization and realizing multiple scans with different angles. Figure 5 depicts the same area colorized according to reflectivity levels as perceived by the system in post-processing. The bright red stripes of area do not represent a real increased reflectivity however, but rather areas of scanning flight overlap that has been incorrectly evaluated by the software as high reflectivity due to a denser point cloud.

The test target is practically invisible in both pictures.

A. *Mapping flight at 50 m altitude*

Fig. 4. Results using both the lidar point cloud and an overlay from photogrammetry at 50 m altitude.

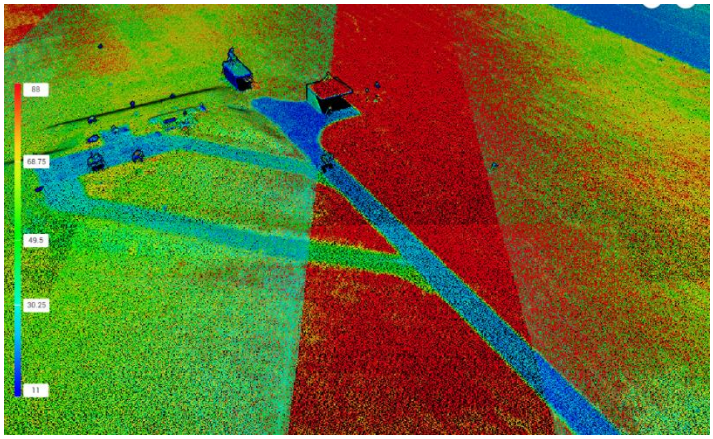

Fig. 5. Colorization according to reflectivity levels obtained from the data.

Fig. 6. Results using both the lidar point cloud and an overlay from photogrammetry at 100 m altitude.

Fig. 7. Colorization according to ground point classification obtained from the data.

B. *Mapping flight at 100 m altitude*

Figure 6 is again an overlap of camera data and lidar point cloud, this time taken from a 100 m altitude. At this range, it becomes nearly impossible to identify the small group of people. Figure 7 shows a different colour mode based on ground-point recognition. The point cloud is colorized in post-process to best differentiate between the ground and all other objects, and sometimes can offer a clearer overview than reflectivity or height mapping.

A different area with a distinct treeline, a road, and several cars was also mapped. Below, in Figure 8 the ground point recognition offers a clear distinction between the forest and cars, it however fails to recognize an asphalt road.
This road is clearly visible in Figure 9, thanks to reflectivity measurement carried out on the same flight. In Figure 9 it is also

worth noting that different reflectivity was detected on different vehicles due to their paint colours.

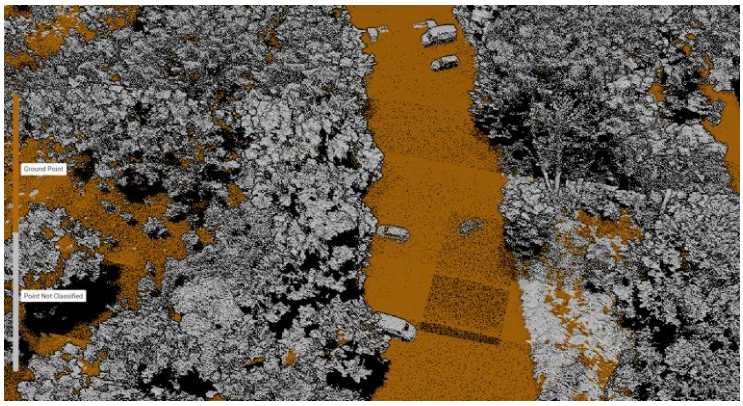

Fig. 8. Ground point recognition in different scene.

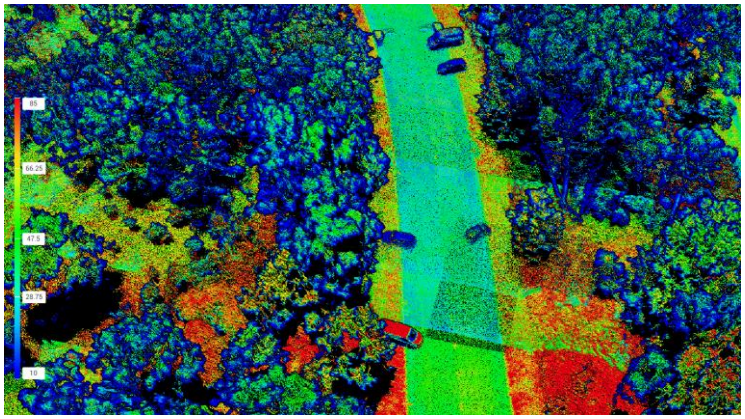

Fig. 9. Colorization according to reflectivity levels obtained from the data.

V. Conclusions

Commercial lidar solutions are becoming ever more widespread and accessible. At an affordable price-point, with an intuitive interface and efficient handling they offer a powerful tool for terrain mapping, autonomous driving and object detection and classification, especially when paired with other sensors like radar and cameras.

It is important, however, to keep the limitations of each system in mind when choosing a solution for a particular scenario. While a lightweight, automotive lidar can offer a fairly reliable mapping of the surrounding area, with distance its resolution can deteriorate far below the manufacturer stated values.

As expected, surface reflectivity had influence on obtained data point cloud density, with bright metallic surfaces reflecting more rays than dark and plastic materials. This effect could be observed on car paint and various tent and buildings materials, but not on the intended test targets, as those proved too small to map regardless of material properties.

During the course of the experiment, the only sensor able to detect the testing target was the RGB camera, with the lidar barely picking up enough cloud points at 50 m distance. Achieved resolution values did not exceed 10 cm in either depth or width.

In general, field-experiment results can rarely achieve the values obtained in a laboratory environment. This experiment was carried out in as near-optimal working conditions for the system as possible given the time of year and local climate. Temperature, humidity levels and light conditions were all within the working range of the system. Wind speed stayed between calm and a light breeze throughout all flights.

From the standpoint of system compatibility, the data obtained from the camera and the lidar highly corresponded, and their overlap in post-processing posed no issues.

Should the 3D data be evaluated by an algorithm, the lidar dataset would likely suffice for object recognition on its own. With a person in-the-loop, however, the colourization provided by the RGB camera proved an added value, making the target area much easier to read to the human eye.

Used lidar system is a typical automotive-grade lidar, therefore mounting it on a UAS may add error to the results, increasing the importance of INS measurements accuracy.

Even so, in the experiment, the lidar system proved effective in mapping the ground elevation and larger objects like trees and vehicles, and at a shorter distance, even people. The interface offered time-effective mission planning and intuitive controls, and required little-to-no additional training for the UAS operator.

For higher resolution object detection and classification, and for larger distances, however, a different, higher energy lidar system would be more appropriate.

Acknowledgment

The authors would like to thank the Exercise Control Team of the NATO Counter – Unmanned Aircraft Systems Technical Interoperability Exercise 2023 (NATO C-UAS TIE 23), for their invaluable support in the realization of the experiment: for providing technical facilities, equipment and a dedicated test area, as well as for their extensive expertise, helpful advice and positive attitude.

References

[1] P. McManamon, “Field Guide to Lidar,” in SPIE Field Guides, vol. FG36, SPIE PRESS, Bellingham, Washington USA, 2015. ISBN: 9781628416558.

[2] L. C. G. David, A. H. Ballado, S. M. Sarte and R. A. Pula, "Mapping inland aquaculture from orthophoto and LiDAR data using object-based image analysis," *2016 IEEE Region 10 Humanitarian Technology Conference (R10-HTC)*, Agra, India, 2016, pp. 1-5, doi: 10.1109/R10-HTC.2016.7906855.

[3] E. J. Welton *et al.*, "The NASA Micro Pulse Lidar Network (MPLNET): Early Results from Development of Diurnal Climatologies," *2021 IEEE International Geoscience and Remote Sensing Symposium IGARSS*, Brussels, Belgium, 2021, pp. 1432-1433, doi: 10.1109/IGARSS47720.2021.9553788.

[4] J. -K. Liu, K. -T. Chang, C. Lin and L. -C. Chang, "Accuracy evaluation of ALOS DEM with airborne LiDAR data in Southern Taiwan," *2015 IEEE International Geoscience and Remote Sensing Symposium*

(IGARSS), Milan, Italy, 2015, pp. 3025-3028, doi: 10.1109/IGARSS.2015.7326453.

[5] L. Holmen, G. Rustad, and M. Haakestad, "Eye-safe fiber laser for long-range 3D imaging applications," Appl. Opt. 57, 6760-6767, 2018.

[6] C. Bodensteiner, W. Hübner, K. Jüngling, P. Solbrig and M. Arens, "Monocular Camera Trajectory Optimization using LiDAR data," 2011 IEEE International Conference on Computer Vision Workshops (ICCV Workshops), Barcelona, Spain, 2011, pp. 2018-2025, doi: 10.1109/ICCVW.2011.6130496.

[7] C. Larat, M. Schwarz, E. Lallier, and E. Durand, "Eye-Safe Q-Switched Er:YAG MOPA Laser System," in Advanced Solid-State Lasers Congress, G. Huber and P. Moulton, eds., OSA Technical Digest (online) (Optica Publishing Group, 2013), paper JTh2A.47.

[8] A. Knigge, A. Klehr, A. Liero, J. Fricke, A. Maaßdorf, A. Zeghuzi, H. Wenzel, and G. Tränkle, "Wavelength stabilized 905 nm diode lasers in the 100 W class for automotive LiDAR," in 2019 Conference on Lasers and Electro-Optics Europe and European Quantum Electronics Conference, OSA Technical Digest (Optica Publishing Group, 2019), paper cb_5_2.

[9] A. Laugustin, C. Canal, and O. Rabot, "State-of-the-art laser diode illuminators for automotive LIDAR," in 2019 Conference on Lasers and Electro-Optics Europe and European Quantum Electronics Conference, OSA Technical Digest (Optica Publishing Group, 2019), paper cb_p_15.

[10] T. F. Refaat *et al*., "Backscatter 2-μm Lidar Validation for Atmospheric CO2 Differential Absorption Lidar Applications," in *IEEE Transactions on Geoscience and Remote Sensing*, vol. 49, no. 1, pp. 572-580, Jan. 2011, doi: 10.1109/TGRS.2010.2055874.

[11] M. Eichhorn, "Laser Physics: From Principles to Practical Work in the Lab," Springer, 2014, ISBN : 978-3-319-05127-7.

[12] C. Kyba, A. Mohar, T. Posch, "How bright is moonlight?" - A&G Astronomy and Geophysics, 58, 1, pp. 1.31—1.32., 2017, doi: http://doi.org/10.1093/astrogeo/atx025.

[13] Livox Avia User Manual, Available online: https://terra-1-g.djicdn.com/65c028cd298f4669a7f0e40e50ba1131/Download/Avia/Livox%20Avia%20User%20Manual%20202204.pdf.